An Investigation of the Redox Stability of an Anode-Supported SOFC Stack Using Acoustic Emission Monitoring

V. H. Rangel-Hernandez[a], U. de Haart[a], Q. Fang[a], D. Schäfer[a], F. Thaler[a], R. Peters[a] and L. Blum[a]

[a] Electrochemical Process Engineering (IEK-14), Institute of Energy and Climate Research, Forschungszentrum Jülich GmbH, 52448, Jülich, Germany

The mechanical stability of an SOFC stack is compromised when its cells operate in oxidation-reduction (Redox) environments. Previous studies, based mainly on voltage-current or electrochemical impedance measurements, showed that cell performance degraded upon redox cycling above 600 °C. Therefore, the purpose of this work is to investigate the Redox process and the stability of a SOFC stack applying the Acoustic Emission (AE) monitoring technique. The investigation includes the interpretation of AE events and signals considering their waveform and frequency content.

Introduction

The current interest in solid oxide fuel cells (SOFC) technology derives mainly from the high power generation/conversion efficiency and low-to-zero emissions (1-2). Their current application in stationary power generation systems attests to their technological maturity. However, the stability and performance of the cells or stacks could be compromised due to the adverse conditions to which they are typically exposed. During the operation of a cell stack, cells are subjected to internal stresses primarily caused by differences in the thermal expansion of the different SOFC materials, by temperature gradients (3-4) and by the oxidation of nickel (Ni) particles found in the Ni-YSZ composites widely used as anode materials in SOFCs (5-6). Although the latter condition often occurs in Ni-based anode-supported cells (ASC) as a result of unplanned reduction-oxidation (redox) cycles, further research is still required.

In practice, the occurrence of a Redox cycle in an SOFC stack has a number of causes, such as a sudden cut in the fuel supply to the stack or a high fuel utilization due to an operating condition. The important thing to note is the irreversible damage it causes to the cells. During a redox cycle, the anode undergoes changes in its volume due to the oxidation of Ni to nickel oxide (NiO), which results in microstructural damages to the anode itself, the electrolyte or to both (5,7).

A previous study showed that the cell performance decreased after redox cycling above 600 °C, mainly based on the voltage-current curve measurements (8). However, only a few papers have reported on the application of the acoustic emission (AE) technique to the study of redox stability (e.g., 5,9-10). Thus, there is currently still concern regarding how best to ensure the mechanical reliability of SOFCs under these particular operating conditions.

This study investigates the redox process and stability of an SOFC stack by applying the AE monitoring technique.

Experimental

Sample Preparation

The experiments were conducted using an SOFC stack previously developed at the Forschungszentrum Jülich (11). Table 1 presents an overview of its main characteristics.

TABLE I. Design of the stack (F1004-113).

	F1004-113
Number of cells	4
Active cell area	80 cm^2
Thickness of anode substrate	300 µm
Anode contact	Ni mesh
Anode	Ni/YSZ
Electrolyte	8YSZ
Barrier layer	CGO
Cathode	LSCF
Cathode contact layer	LSCF (screen printing)
Protective coating	MCF (APS)
Sealant in stack	Glass H (Jülich)

AE Monitoring equipment

The acoustic monitoring was carried out using AMSYS-6 equipment from Vallen Systeme Gmbh (12). This consisted of four AE preamplifiers (AEPH5) with a gain of 34 dB at 50 ohm and four wideband AE sensors (VS160-NS) with a frequency range from 100-450 kHz. The acquisition parameters set in the AE equipment are presented in Table 2.

TABLE 2. Acquisition parameters.

	Value
TR data sample rate	5 MHz
AE data sample rate	10 MHz
Threshold	50 dB
Pre-trigger samples	200 µs
Preamplifier gain	34 dB
Digital filter	95 kHz – 850 kHz

Figure 1 displays the assembly of the AE monitoring system and SOFC stack. It can be seen that 0.03-m long steel waveguides were used to fix the sensors in the stack. Figure 2 shows a schematic that details the position and identification of the sensors therein. To improve the sensitive response of the sensors, vacuum grease was applied as a coupling agent between the sensors and the base of the waveguides. To verify the correct installation of the AE sensors, a pencil-lead break test was carried out (13).

Figure1. Assembly of AE equipment and SOFC stack.

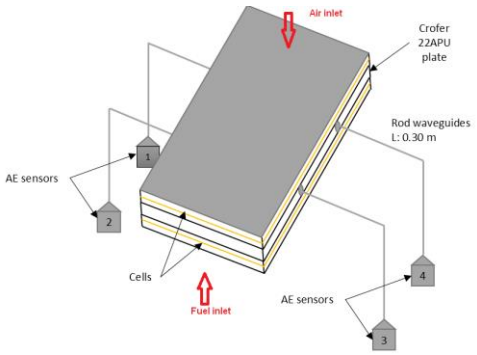

Figure 2. Schematic of AE sensors localization in stack.

Experimental procedure

The stack was heated to typical operating temperature of 700 °C with H_2 (0.16 slm) and Ar (3.84 slm) supplied to the anode side, and air (4 Nl/min) supplied to the cathode side. Before each of the redox cycle, the OCV operation was performed at 700 °C with H2 (4.5 slm) and air (16 slm). After at least two hours, the current-voltage (I-V) characteristic curves at 700 °C were generated.

Subsequently, the redox cycles were implemented at 625°C according to the following procedure. This consisted, initially, of cooling the stack to the indicated temperature using H_2/Ar (0.16/3.84 slm) as the reducing gas and air (4 slm) as the oxidizing medium. The anode was first purged with Ar (2 slm). It was then oxidized by applying air (0.5 Nl/min) to the anode side, as the amount of air supplied to the cathode was maintained. Afterwards, the stack was flashed again with pure Ar. Finally, the initial values of the gases were restored and the stack was heated back up to 700 °C for characterization.

In the meantime, the AE monitoring system, through the Vallen Software (12), was used to collect all of the raw data generated during the tests. This enabled a parametric analysis of the measurements to be conducted. The signal processing was then performed using the Origin software (14).

Results and Discussion

Figure 3 depicts the evolution over time of some of the operating parameters of the stack, most notably the cell voltages and operating temperature. The plot shows that the stack was in operation for about 4300 hours. Subsequently, in an attempt to determine possible leakage and changes in cell performance, the OCV (Figure 4(a)) and cell voltage at 0.4 A/cm^2 (Figure 4(b)) were recorded and compared at operating temperature via the number of redox cycles.

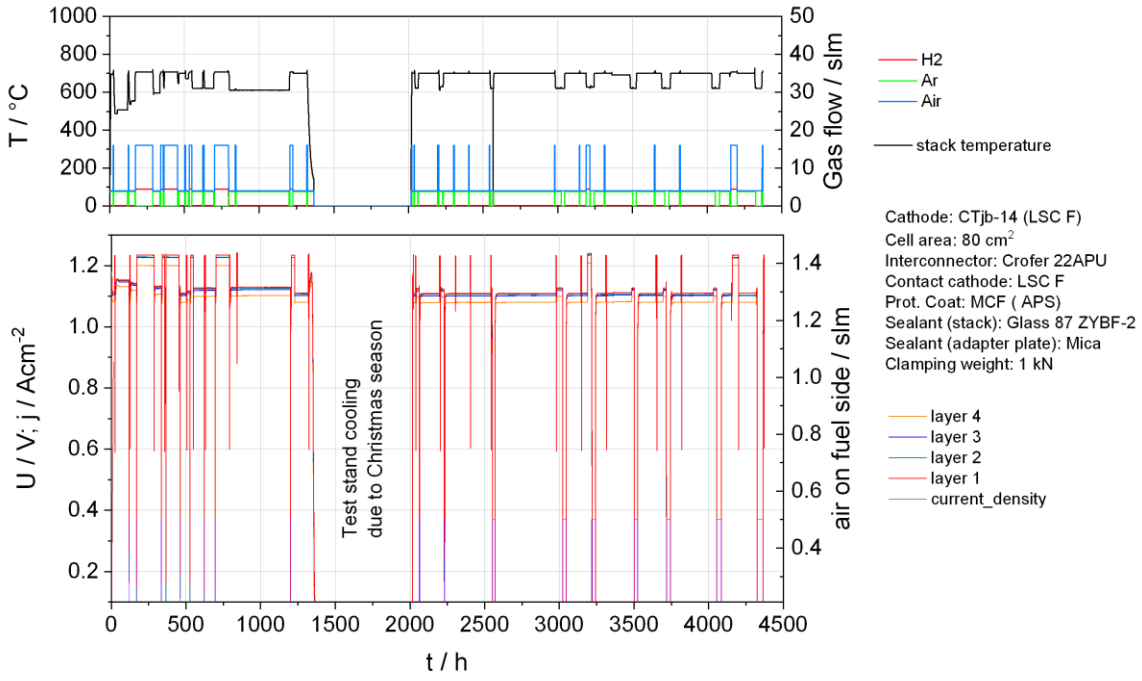

Figure 3. Evolution of the cell voltage and stack temperature over ca. 4300 h.

With respect to the OCV of the stack, no visible change was observed after the 13-redox cycles in which the stack was tested. It was therefore assumed that no substantive change occurred in terms of the gas tightness of the cells. However, a notable decrease in the electrochemical performance of the cells was observed in the results. Layer 4 had a drop of 11%, layers 1 and 3 of 11.5%, and finally layer 2 a decline of 12% with respect to the reference value (marked in the graph as 0).

Figure 4(b) also shows the time that each of the redox cycles lasted at 625 C. As a general observation, it was noted that the largest drops in performance mostly occurred following cycles with the longest duration, especially those lasting 18 and 23 hours.

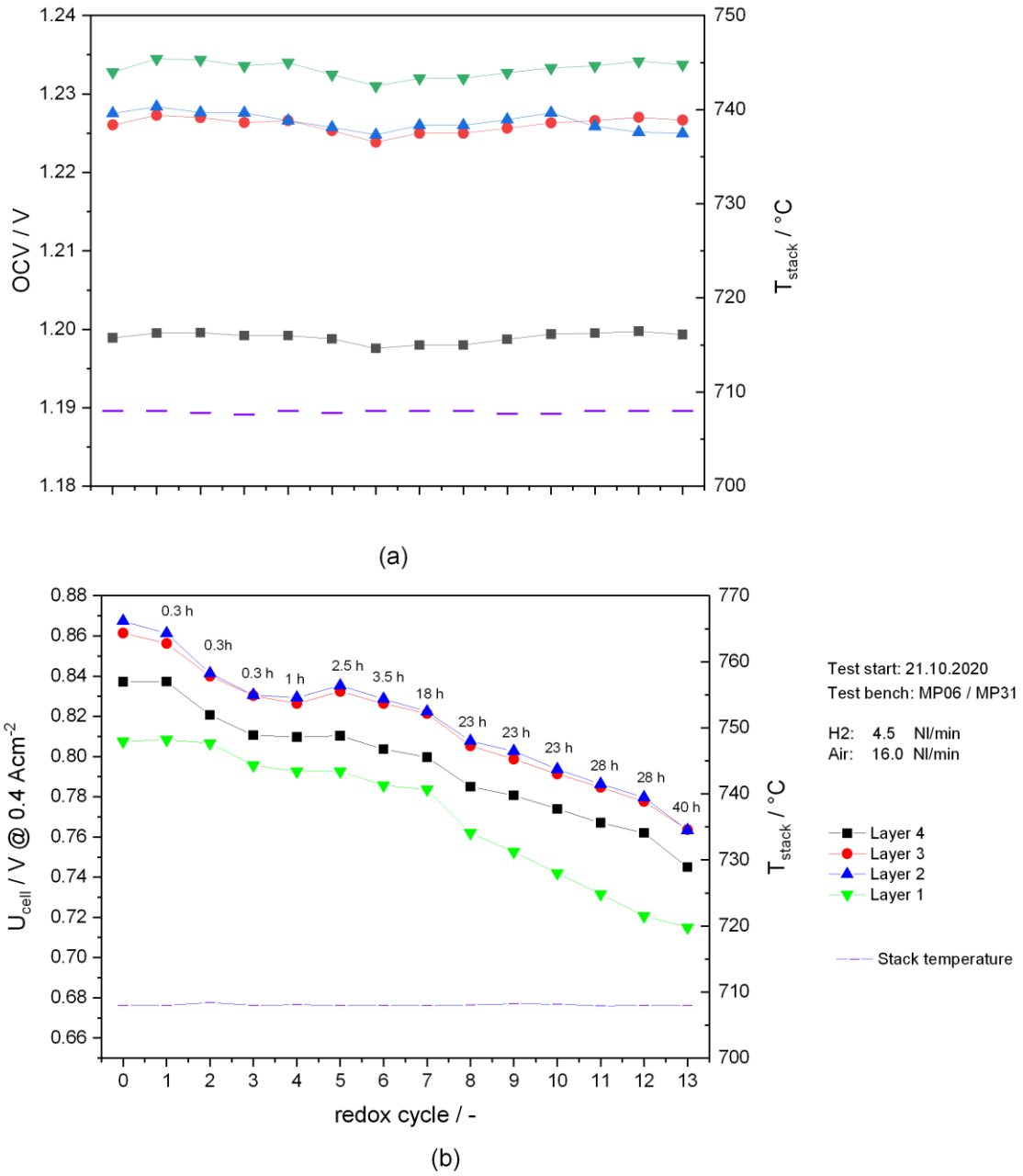

Figure 4. a) OCV of the cells depending on the number of redox cycles and b) cell performance after the redox cycles at 700 °C.

For the following acoustic emission analysis only one of the redox tests has been considered. It was test number 8 with a duration of 23 hours, as is shown in Figure 5(a). The lines correspond to the voltages of the different cells of the stack, whereas the colored-dots indicate the acoustic events detected by the sensors. Here, two distinct stages were clearly visible in which most of the AE events arose: the first was during the oxidation of Ni to NiO and the second in accordance with the reduction of the NiO. This was reproducible in all 13 cases analyzed. On the other hand, over the period in which the voltage remained stable at zero, no significant acoustic emission was detected. Only

electromagnetically-induced noise signals were detected (circles marked in red) [15], which prompted a classification of the signals, as shown below.

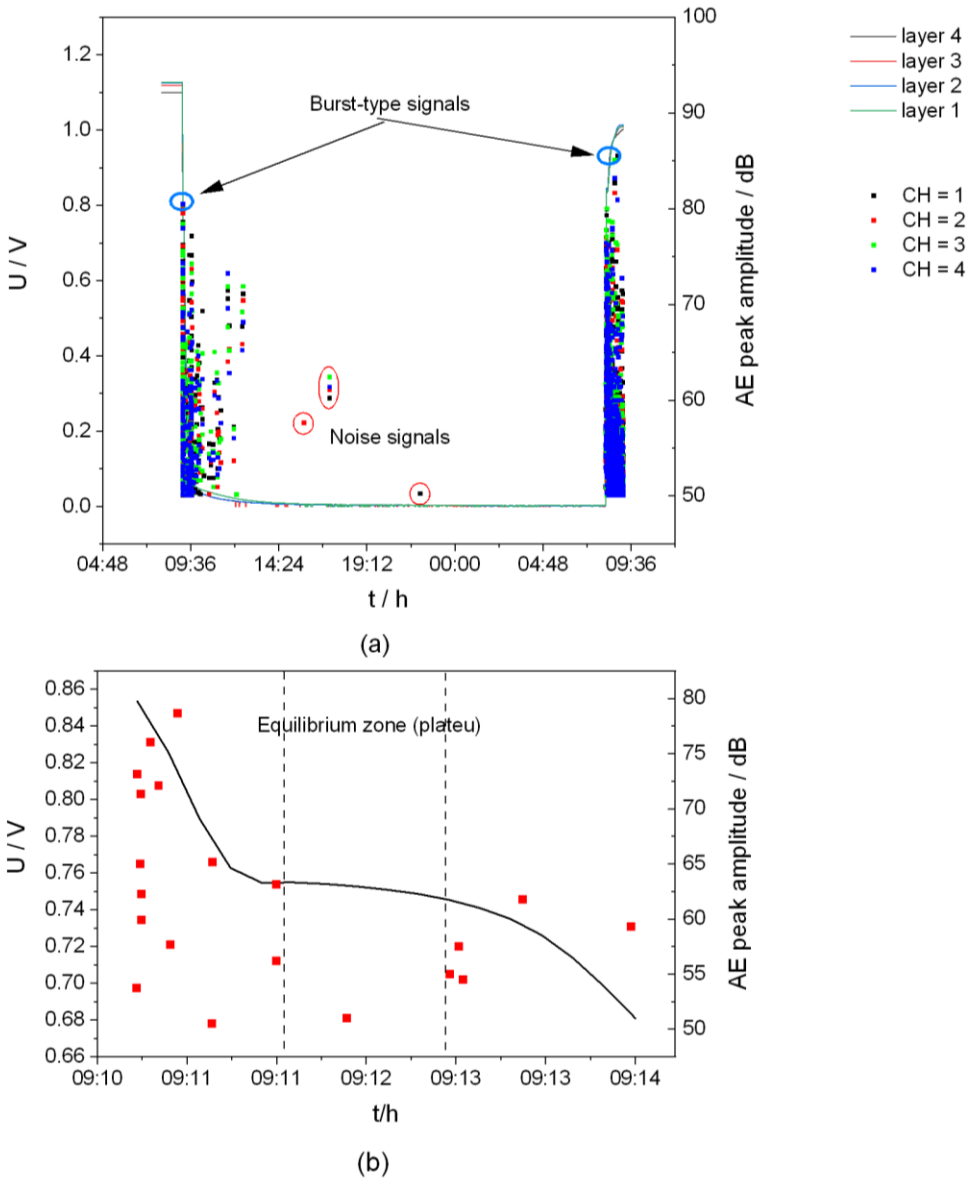

Figure 5. a) AE peak amplitude and cell voltage over redox tests at 625 °C; and b) AE events in the redox equilibrium zone.

A further interesting finding was the analysis of the Ni/NiO equilibrium stage, as shown in Figure 5(b). Especially at this stage, a considerable decrease in AE events was observed, which was reproduced in the remaining tests. This could be explained by the fact that at this stage, in spite of the volume expansion that accompanies the oxidation of Ni to NiO, no significant distortions are generated inside the electrode that cause mechanical and therefore acoustic energy release. Following this equilibrium, the number of acoustic events considerably increased again.

Signal-based analysis

The number of AE signals generated during the test was very large, and therefore the following analysis only refers to burst-type signals, as these were more likely to be attributed to one type of damage source [15]. For this purpose, two burst-type signals (marked in blue circles) were extracted from the data shown in Figure 5(a). Thus, Figure 6 reveals the features of the AE signal samples in the time and frequency domains.

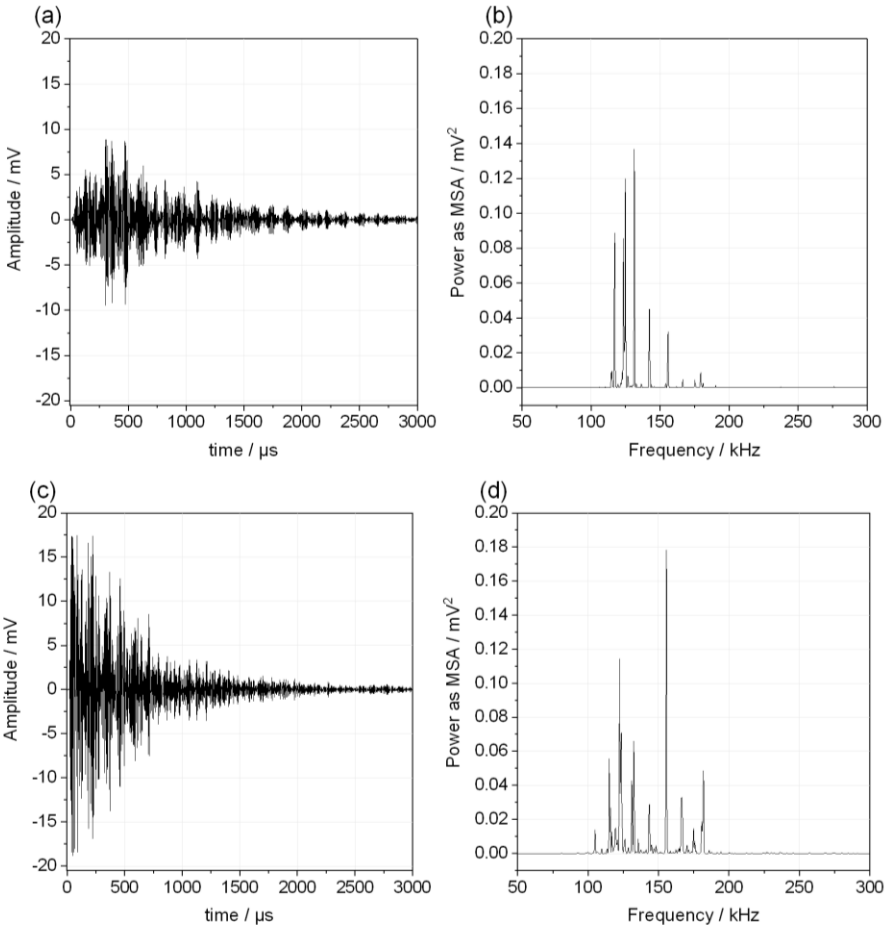

Figure 6. Extraction of features from two sample AE signals in time and frequency domain: a-b) onset of oxidation stage and c-d) end of reduction stage. .

The first signal pertains to the onset of the oxidation stage, with its waveform representing a burst-type signal with a low amplitude (< 10 mV) decaying in time, as shown in Figure 6(a). By analyzing its power density, it was possible to observe that most of the frequency peaks were below 170 kHz. Only a few spikes of very low power were revealed at frequencies above 170 kHz. Figure 6(c), in contrast, shows a signal that was drawn from the end of the reduction stage. Its waveform provides evidence that the signal could fall within the region of interest. That is, its origin may be mechanical damage due to shrinkage of the particle volume at the anode, i.e. release of internal stresses. However, work is still underway to corroborate these findings.

Conclusions

In this study, an anode-supported cell stack was subjected to redox thermal cycling. This yielded interesting results. On the one hand, at an operating temperature of 625°C the redox cycles caused a notable degradation in the performance of the cells. On the other, acoustic monitoring of the redox tests indicated possible acoustic events due to microstructural damage in the cell, but thus far no certainty as to the origin of these events has been established. However, this allows us to suggest a possible correlation between the degradation of the cells and the acoustic events found here, and so this hypothesis is still being developed.

Acknowledgments

The authors gratefully acknowledge Mr. Stefan Küpper for the preparation of the fuel cell stack test bench, and Dr. M.G.R. Sause for his helpful discussions and advices about AE monitoring.

References

1. A.L. Dicks and D.A.J. Rand, *Fuel cell systems explained.* Wiley Interscience, New Jersey (2018).
2. H. Monzón and M.A. Laguna Bercero, *J. Phys. Energy*, **2**, 014005 (2020)
3. A. Atkinson and B. Sun, Mater. Sci. Tech., **23**, 1135 (2007)
4. L. Blum, S.M. Groß, J. Malzbender, U. Pabst, M. Peksen, R. Peters, L.C. Vinke, *J. Power Sources*, 196, 7175 (2019).
5. K. Kumada and K. Sato and T. Hashida, *ECS Trans.*, **78**(1), 2355 (2017).
6. D. Sarantaridis and A. Atkinson, *Fuel Cells*, 7(3), 246 (2007).
7. A. Faes, A. Nakajo, A. Hessler-Wyser, D. Dubois, A. Brisse, S. Modena, J. Van herle, *J. Power Sources*, 193, 55 (2009).
8. U. Packbier, T. Bause, Q. Fang, L. Blum, D. Stolten, *12th European SOFC & SOE Forum 2016*, Lucerne, Switzerland, 5-8 Jul (2016).
9. H. Lin, C. Ding, K. Kumada, K. Sato, Y. Tsutai, C. Wada and T. Hashida, *AIP Conference Proceedings*, 987, 163 (2008).
10. K. Kumada, K. Sato and T. Hashida, *16th International Conference on Nanotechnology Proceedings*, Sendai, Japan (2016).
11. Q. Fang, L. Blum, R. peters, M. Peksen, P. Batfalsky, D. Stolten, *Int J Hydrogen Energy*, 40, 1128 (2015).
12. Vallen Systeme GmbH. 2017.
13. M.G.R. Sause, J. Acoust. Emiss. 29, 184 (2011).
14. Origin(Pro), Version 2020. OriginLab Corporation, Northampton, MA, USA.
15. M.G.R. Sause, *In Situ Monitoring of fiber-reinforced composites.* Springer, International Publishing, Switzerland (2016)